CURRENT WORK AT THE FRENCH D.M.N.: KALMAN FILTER, VARIATIONAL ANALYSIS AND SATELLITE DATA IMPACT STUDY

P. Moll, Y. Durand, M.-C. Pierrard, Ph. Caille, P. Betout
Direction de la Météorologie Nationale
Paris, France

Summary: This article describes the current work at the French D.M.N. on the relevant topics for the "Data Assimilation and the Use of Satellite Data" E.C.M.W.F. seminar. Four independent studies are presented. The first one is an application of the Kalman filter to a vertical primitive equation model. The second study exemplifies the difficulties to implement an operational variational analysis. The third study is an example of an application for the variational methods; the goal to be achieved is satellite temperature profile retrieval. The last study is a satellite data impact study in a mesoscale scheme.

1 INTRODUCTION

As the E.C.M.W.F. seminar is dedicated to deal with data assimilation and the use of satellite data, the relevant studies performed by the French D.M.N. data assimilation team are presented. Some of them are not yet finished, and the goal of the present paper is essentially to present the current state of the works under way.

Four independent studies are presented and any chapter can be read independently of the others. The second chapter is

an application of the Kalman filter to a primitive equation spectral (21 waves on the horizontal) ten level two dimensional model. Some results on the error structures and their time evolution are given. The complete presentation can be found in the paper by Moll and Durand (1987), available in French only. The third chapter shows the (small) progress of a weather numerical project including a three dimensional variational analysis. The general theory is given in the paper by Courtier (1987). The main difficulties are listed but the feasibility study must be carried on. The fourth chapter shows how variational methods can be used to retrieve a vertical profile of temperature and humidity from observed raw radiances. A complete description can be found in the paper by Moll (1988), available in French only. The fifth chapter corresponds to a satellite data impact study in a mesoscale data assimilation scheme; several data sets are compared and some preliminary results are shown. A paper on this subject will be submitted to a meteorological review.

2 AN APPLICATION OF THE KALMAN FILTER TO A VERTICAL MODEL

2.1 Introduction

In many meteorological centres, the technique used for data assimilation is the objective analysis based on optimal interpolation coupled with a weather prediction model (e.g. Lorenc, 1981). This method explicitly uses the statistical structures of the prediction errors, but these structures are

quite empirically modelled. The time evolution of these structures relies mostly on intuition.

The Kalman filter is an approach which combines the error statistics and their time evolution due to the dynamic part of the model. This method is a four dimensional generalization of the optimal interpolation, and the time evolution of the prediction errors will be supposed to be determined by the linear tangent model (because of the non linearity of the model).

First, the experimental vertical model is described. Then, some general ideas about the Kalman filter theory are recalled. Lastly, some results are presented as experiment outputs.

2.2 The vertical model

The dynamic part of the study is an adiabatic forecast model in a vertical periodic plan with 9 non equidistant pressure levels. It is a Fourier spectral primitive equation model (see Lepas et al., 1977). The basic equations are :

$$\frac{\partial u}{\partial t} = - u.\frac{\partial u}{\partial x} - w.\frac{\partial u}{\partial p} - \frac{\partial Z}{\partial x} + \mu_u.\frac{\partial^2 u}{\partial x^2} \; ;$$

$$\frac{\partial T}{\partial t} = - u.\frac{\partial T}{\partial x} - w.\frac{\partial T}{\partial p} + \frac{R\,.T}{C_p\,p}.w + \mu_T.\frac{\partial^2 T}{\partial x^2} \; ;$$

$$\frac{\partial w}{\partial p} = - \frac{\partial u}{\partial x} \qquad ; \quad dZ = - RT\, d(\log(p)) \; ;$$

and for the lowest level :

$$\frac{\partial Z}{\partial t} = - u.\frac{\partial}{\partial x}(Z - H) + \frac{R\,T}{p}.w + \mu_Z \frac{\partial^2 Z}{\partial x^2}$$

where u and w are the horizontal and vertical wind components, p is the pressure, H is the orography, T is the temperature, Z is the geopotential height, t is the time, R is the gaz constant, C_p is the thermodynamic coefficient, μ_u and μ_T, μ_Z, are horizontal diffusion coefficients.

The spatial discretization is shown on figure 1. The truncation is spectral with a triangular truncation at wave 21 (equivalent discretization on 64 grid points). A coarser resolution was used if the impact on the results was negligible. The temporal discretization uses a Matsuno explicit scheme.

The model was implemented and validated with an orography corresponding to a 2 km high gaussian mountain. Figure 2 shows the orography and the wind initial conditions.

2.3 The Kalman Filter

The Kalman filter theory is known in meteorology thanks to earlier publications, e.g. Ghil et al. (1980) or Cohn and Parrish (1985). The method consists in estimating both the state of the atmosphere through the assimilation

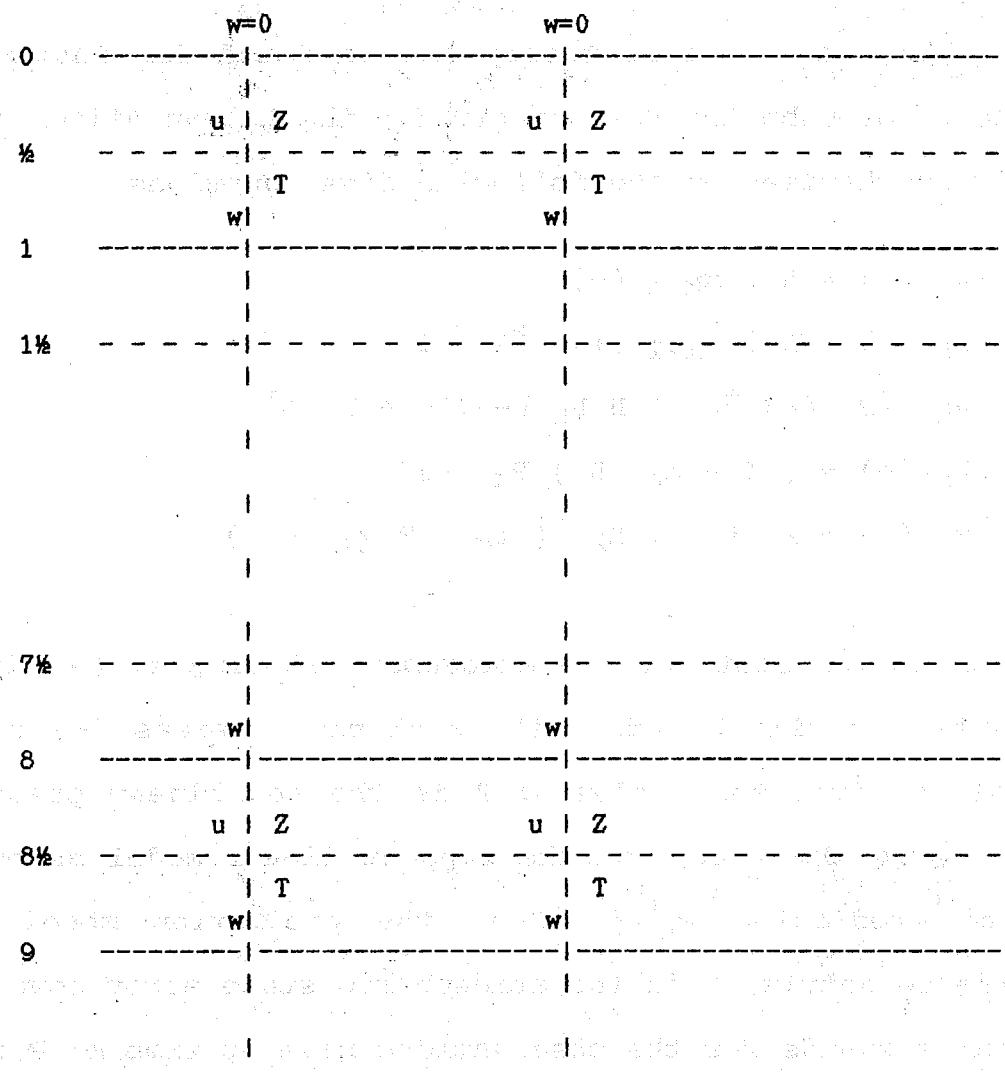

Figure 1 : grid corresponding to the spatial discretisation

system and the error covariances relative to this state for each assimilation time step.

The mathematical theory can be found for instance in the paper of Cohn and Parrish (1985); the Kalman filter scheme can be synthetized by the following five equations:

$$x_k\ (-) = A\ .\ x_{k-1}\ (+)$$

$$P_k\ (-) = \hat{A}\ .\ P_{k-1}\ (+)\ .\ {}^t\hat{A} + T$$

$$K_k = P_k\ (-).\ {}^tH.\ (\ H.P_k\ (-).\ {}^tH + R\ )^{-1}$$

$$P_k\ (+) = (\ I - K_k\ .H\ )\ P_k\ (-)$$

$$x_k\ (+) = x_k\ (-) + K_k\ .(\ z_k - H.x_k\ (-)\ )$$

where x is the state of the atmosphere at time k; (-) denotes the state at time k before the analysis, whereas (+) denotes the state after the analysis; A is the non linear prediction model, $\hat{A}$ is the matrix of the tangent linear model associated to the prediction model; T is the prediction model error covariance matrix; P is the atmospheric state error covariance matrix; z stands for the observations made at time k; R is the observation error covariance matrix; H is the linear link operator between the observations and the atmospheric state; K_k is the objective analysis weight matrix at time k (also called Kalman filter), I is the unity matrix and the letter t denotes the matrix transpose.

This set of five equations is sufficient to assimilate the data and to forecast the error covariances. As the prediction model is rather sophisticated, A is not explicitly determined, but the model is first linearized around the

current equilibrium state (such "linear" states will be deduced as results of the non linear version model at each time step), and the adjoint equations are deduced from the discretized linearized direct equations. This writing requires a great attention, because any error will induce a divergence for the scheme, but this way avoids to handle huge matrices.

Of course, the method proves successful when the prediction model is linear. As our prediction model is non linear, the method would work correctly only if the time evolution of the prediction errors are determined by the tangent linear model (see Lacarra and Talagrand, 1988). This condition has been checked with the vertical plan model, and the whole system was validated.

Several experiments were carried out to test the error behaviour. The main results are given in the next paragraph.

2.4 Main results

2.4.1 Correlation dimensional separability

The correlation dimensional separability is commonly assumed in operational analysis schemes. This hypothesis means that the prediction error correlation between any pair of points is the product of a vertical correlation by a horizontal correlation as shown on figure 3.

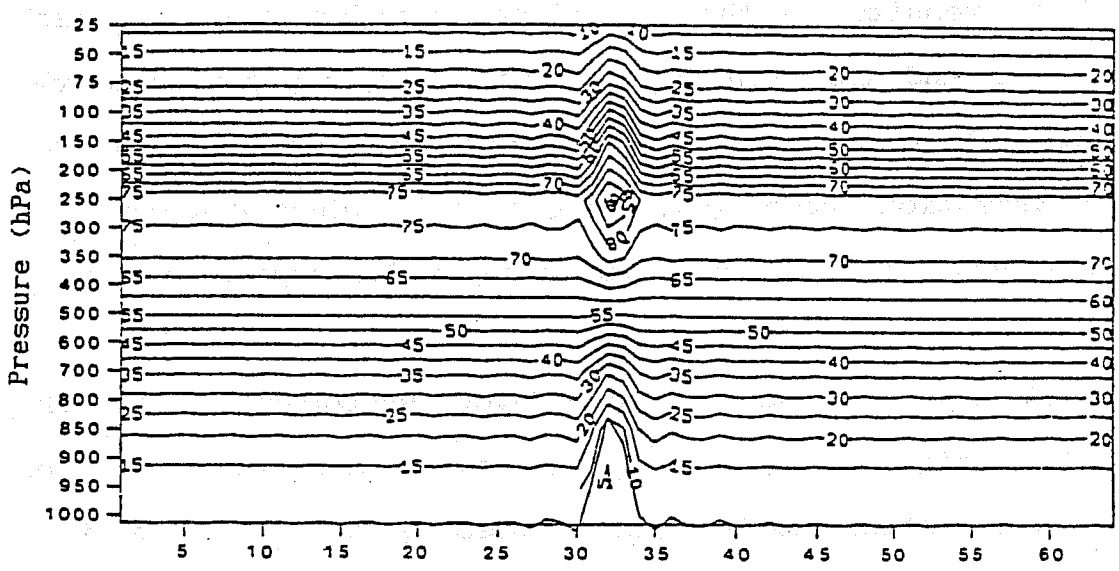

Figure 2 : initial horizontal wind speed field with a 2000m high orography.
the horizontal axis represents the collocation grid points corresponding to 22 waves in the Fourier space.

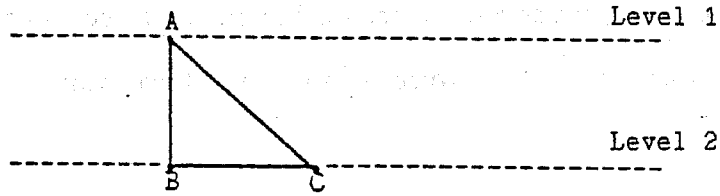

cor(A,C) = cor(A,B) x cor(B,C)

Figure 3 : correlation between any couple of points.

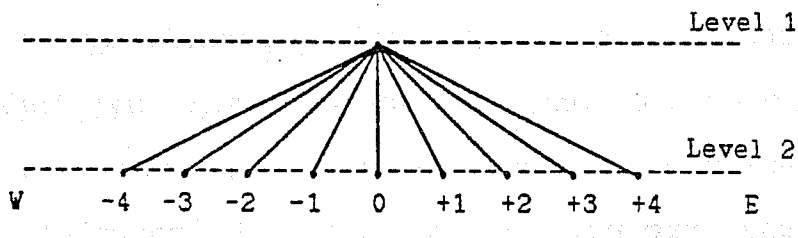

Figure 4 : spatial representation of the grid points for which correlations are to be evaluated.

In order to check this assumption, the correlation between a point of a given level and nine points located on a lower level (see figure 4) are evaluated after several steps of time integration. The computations were made with a T10 truncation, since this coarse resolution does not change the results. Figure 5 corresponds to the maps of correlation for the layer 700/950 hPa after 6 hours of integration : one endorses the separability assumption, the other one does not. The two slant lines represent the eastern and western surface level limits of the orography. After a 12 hour integration, the differences have dramatically increased, as seen on figure 6. The separability assumption seems to systematically under-estimate the correlation (probably because any correlation is evaluated as a product of two correlations, which contributes to decrease the final correlation).

As a consequence, the correlation dimensional separability assumption does not seem to fit in with the true behaviour of error structure. This reveals a weakness in many analysis schemes.

2.4.2 Error correlation spatial structure

Another phenomenon can be seen on figure 6: the correlation between two locations does not vary monotonously with the distance between the locations. That means there is a shift of the correlation maximum value. In order to state this fact more precisely, the error auto-correlations between an

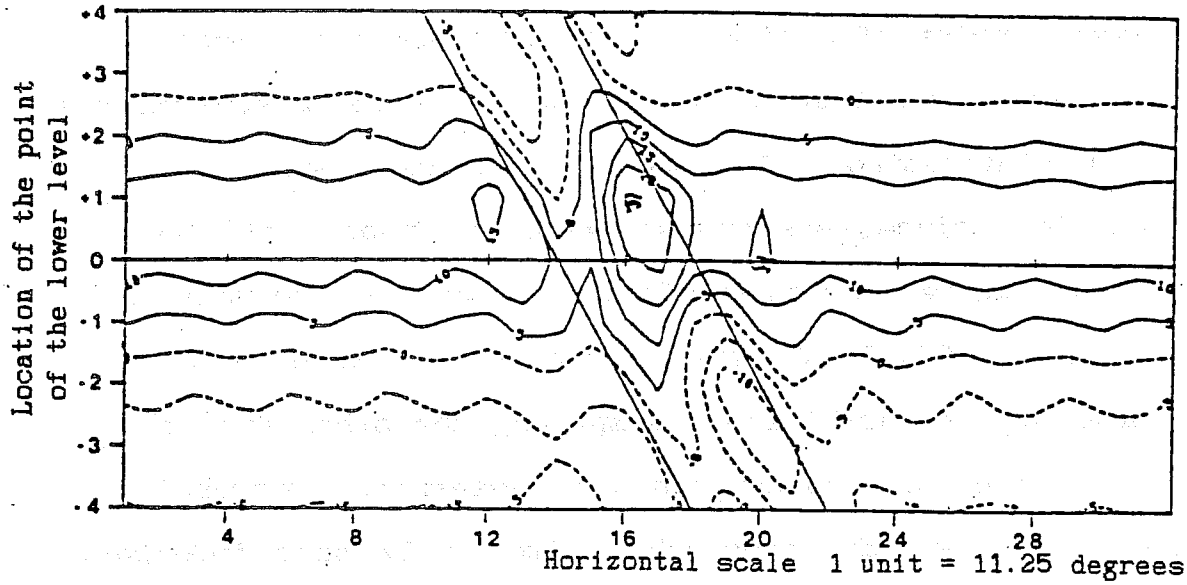

Figure 5 : - horizontal wind speed error correlation (in 1/100) for the 700/950 hPa layer after 6 hours of integration without the dimensional separability hypothesis.

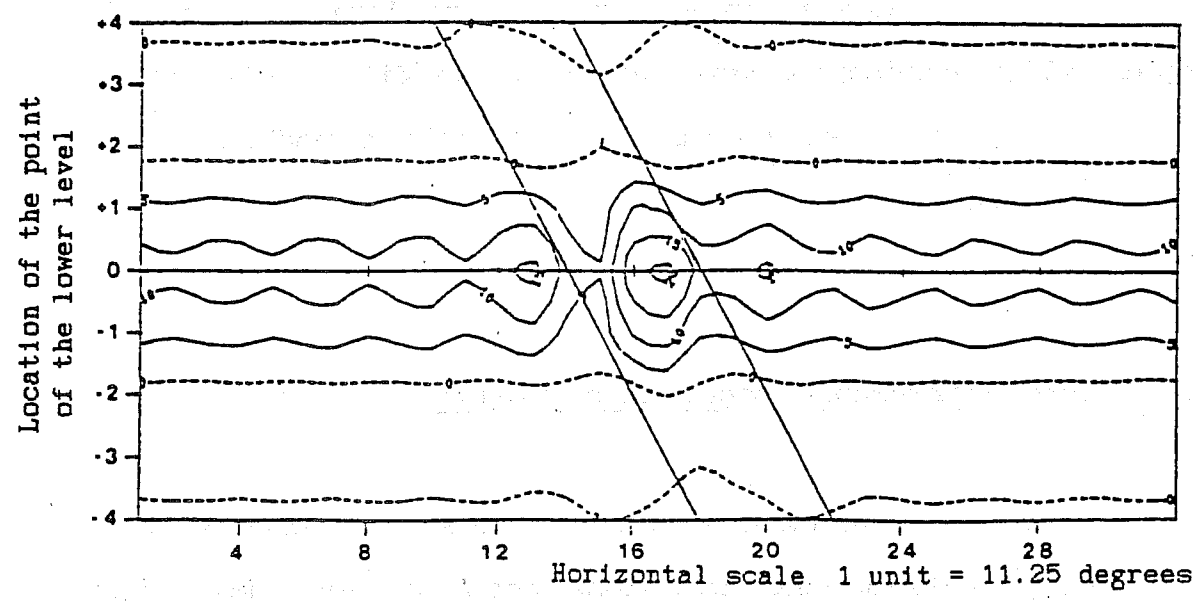

- ut supra with the dimensional separability hypothesis.

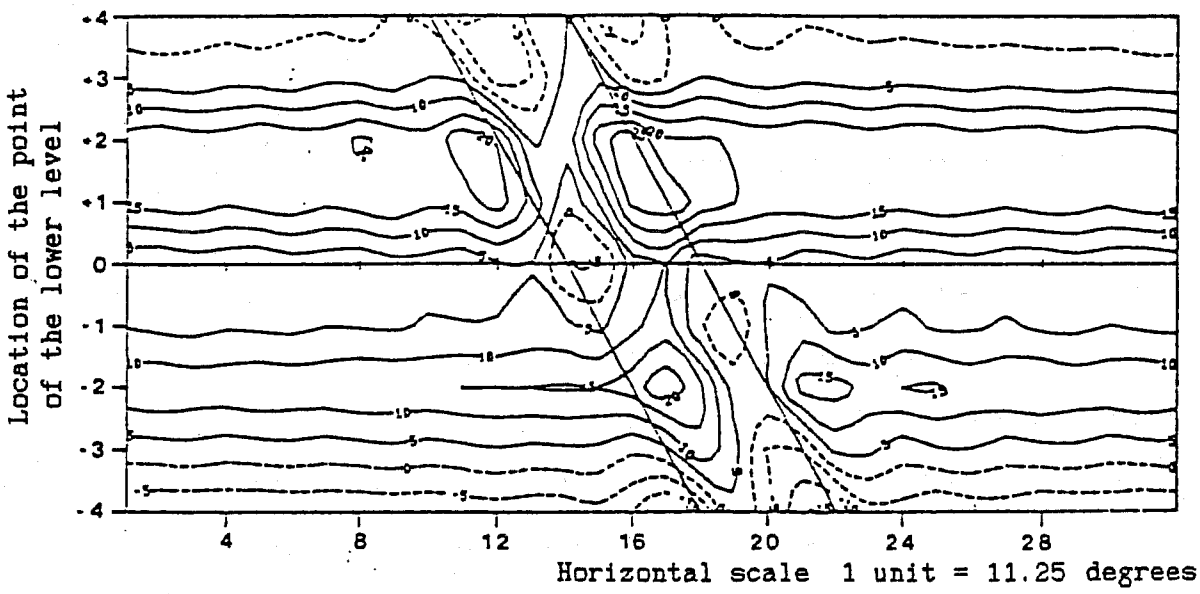

Figure 6 : - horizontal wind speed error correlation (in 1/100) for the 700/950 hPa layer after 12 hours of integration without the dimensional separability hypothesis.

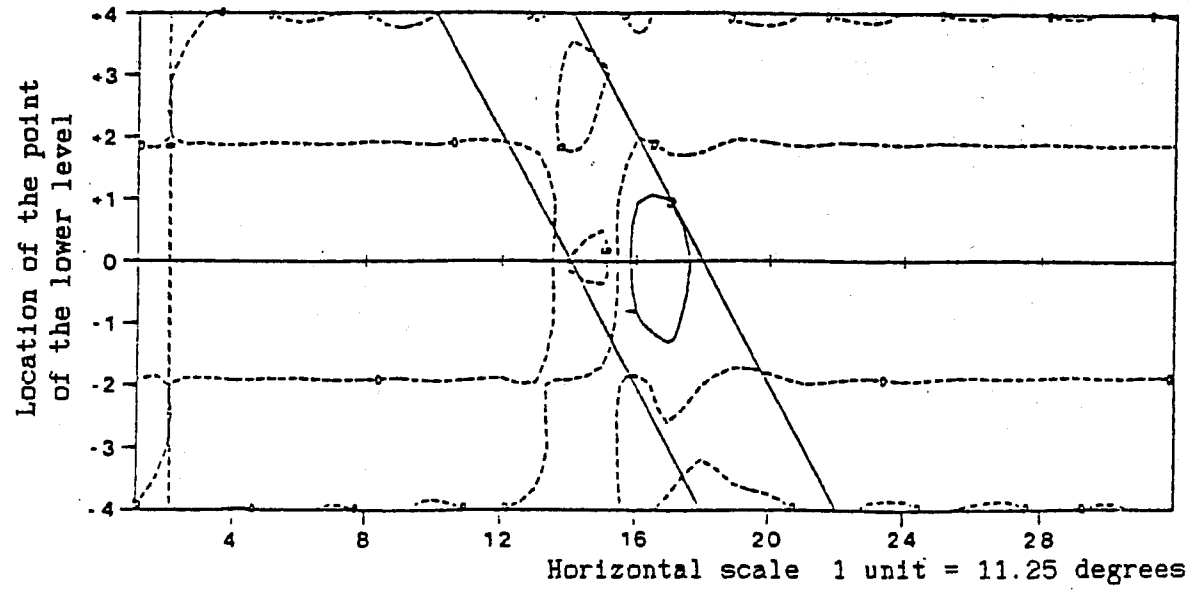

- ut supra with the dimensional separability hypothesis.

arbitrarily chosen location and all the other points were evaluated.

The computations were performed with a T10 truncation. Figure 7 shows the initial correlation for the horizontal wind field with respect to a point located on the 350 hPa level (with the separability hypothesis used only for initialization). After a 12 hour integration of the assimilation scheme, a shift can be noticed for the vertical correlation on the figure 8. The results are qualitatively the same for all the other levels, with however some slight distorsions near the orography at low levels.

Similar results are obtained for temperature error auto-correlations, but the distorsion axis is quite different. This can be seen on figure 9. A similar feature had already been the subject of theoretical studies on the atmospheric fields (e.g. Simmons 1985), but this is rather new for the error structure.

Our assimilation scheme can generate an error statistical structure time evolution corresponding to Kelvin-Helmoltz waves, whereas the current operational schemes cannot.

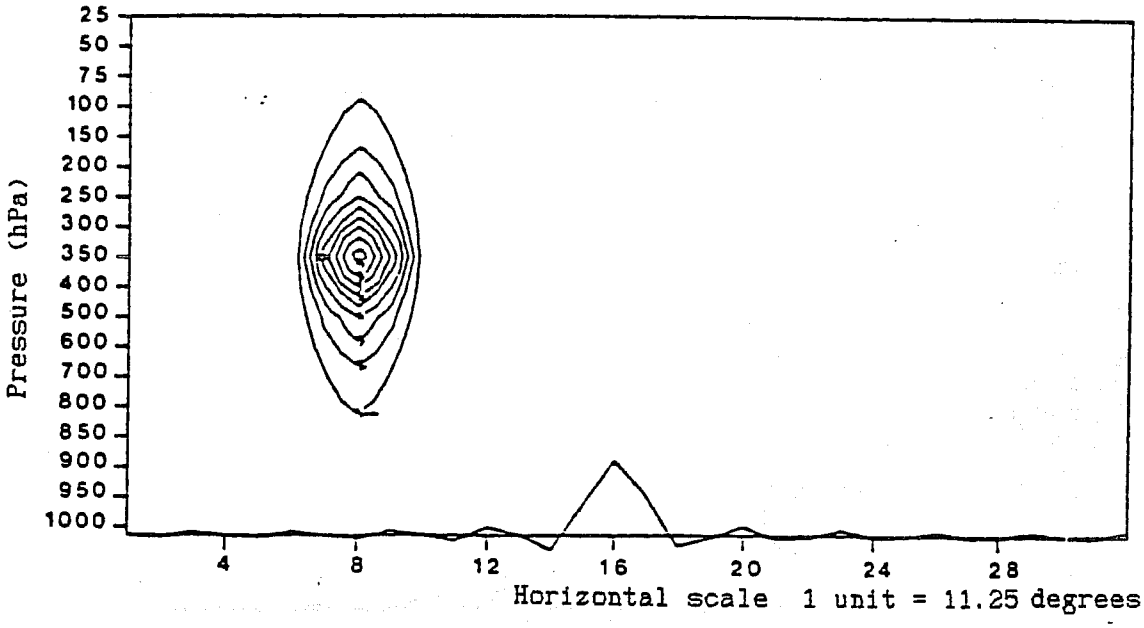

Figure 7 : initial horizontal wind speed error correlation (in 1/100) between the 8th grid point on the 350 hPa pressure level and all the other grid points.

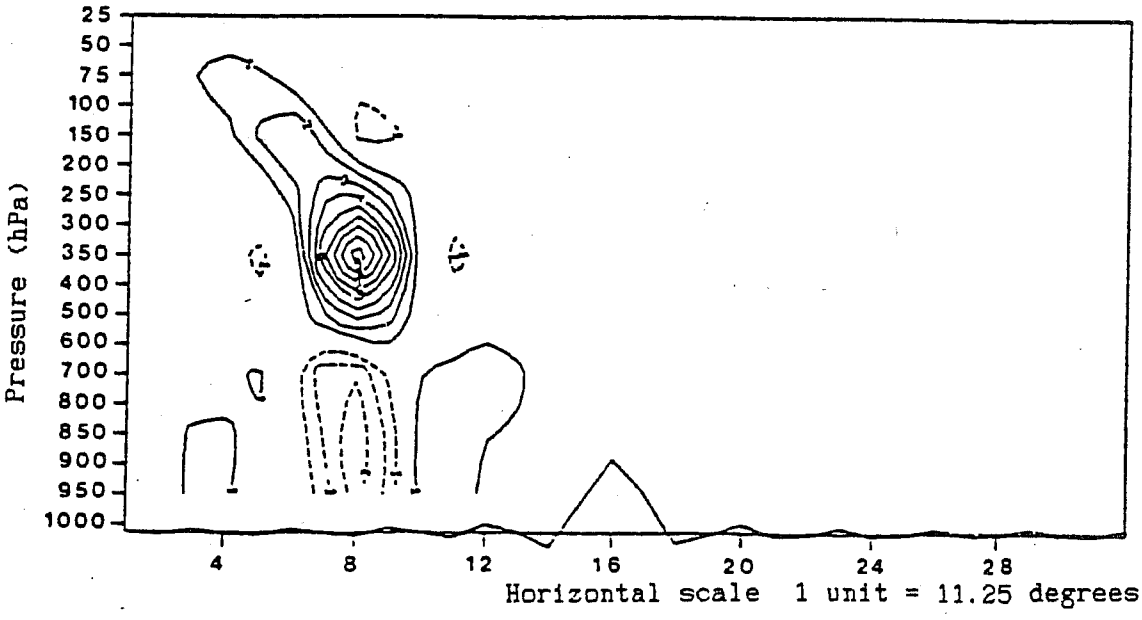

Figure 8 : as in Figure 7 after 12 hours of integration.

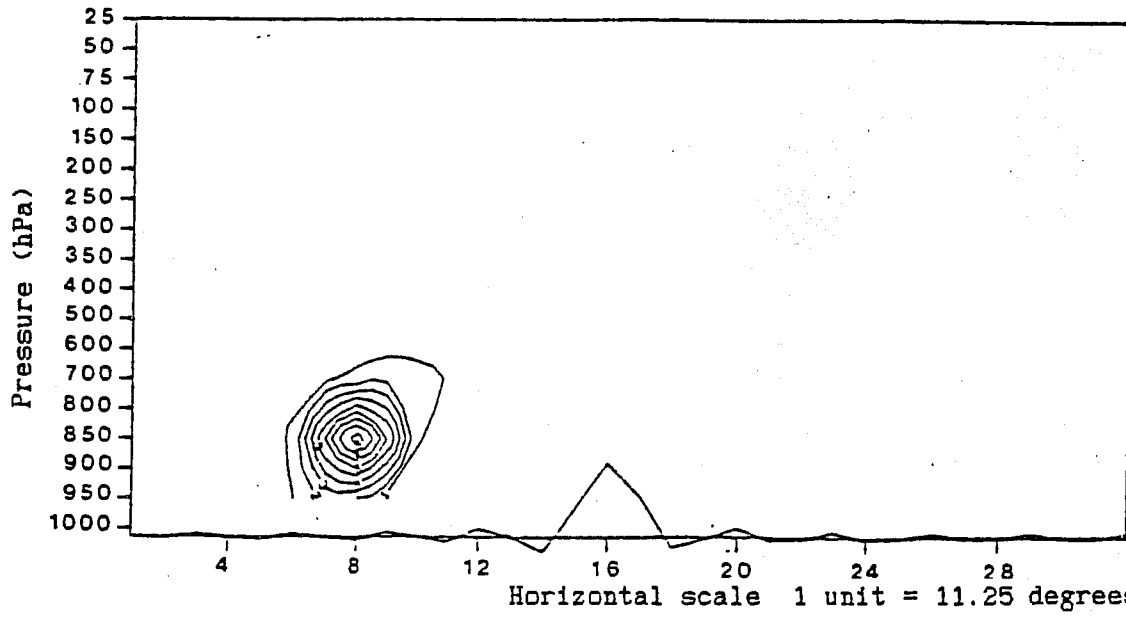

Figure 9 : temperature error correlation (in 1/100) after 12 hours of integration between the 8th grid point on the 850 hPa pressure level and all the other grid points.

2.4.3 Observation impact on error statistics

The goal of this last experiment is to estimate the impact of observed data on error statistics. A first experiment was carried out with a T10 truncation where a radiosonde was simulated to deliver temperature and wind information on a complete profile every three hours.

A basic feature of the assimilation scheme is the propagation of the information. Moreover, our scheme is able to make the error structures evolving. With a radiosonde, the horizontal propagation is noticed on figure 10 after 6 hours of integration. The error variances are lower in the vicinity of the radiosonde (grid point 12) and the eastward propagation is obvious.

The results for the wind and temperature error structures are rather similar, but the different tilt of the axis is visible again, as mentioned in the previous part (see figure 11).

Another experiment was carried out with simulated AIREP reports. As they are single level observations, it was possible to exhibit both a horizontal and a vertical propagation of the information.

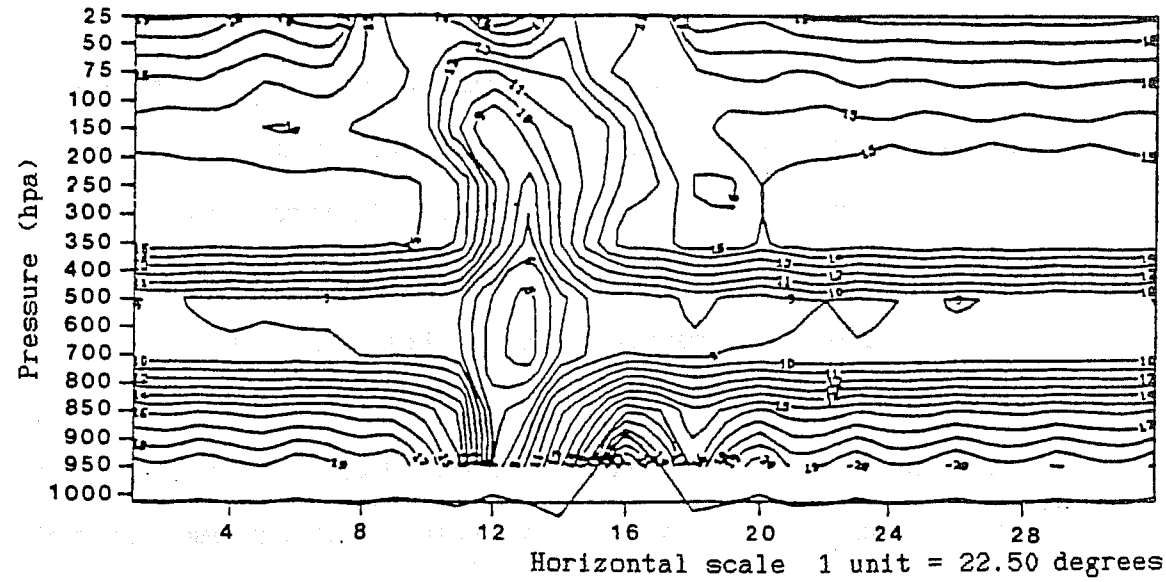

Figure 10 : wind speed error variance (in $m^2.s^{-2}$) after 6 hours of integration with a simulated radiosonde located on the 12th grid point.

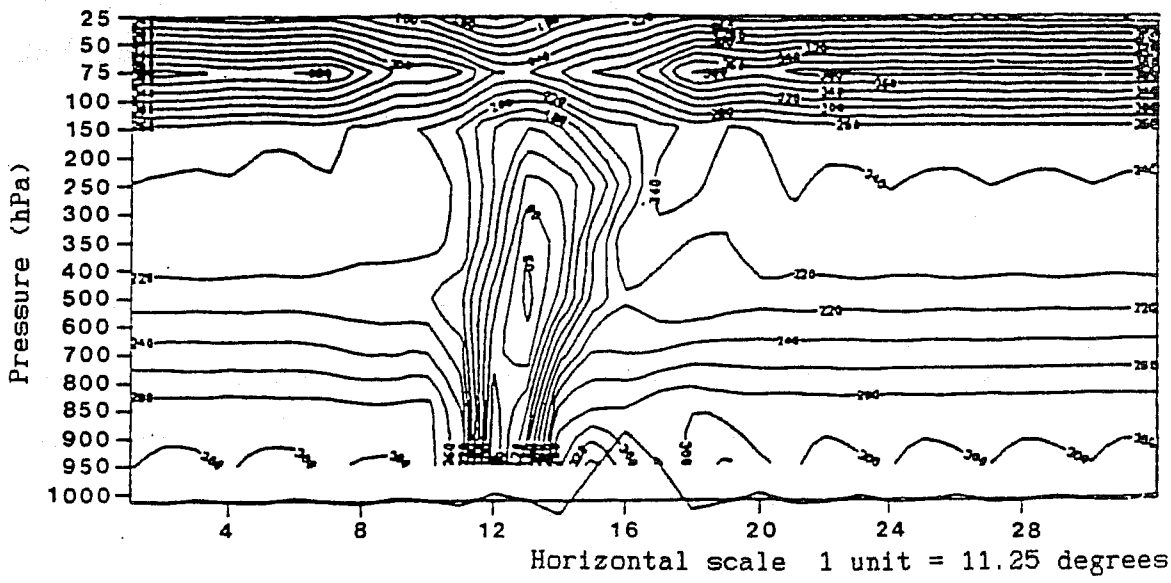

Figure 11 : as in Figure 10 for the temperature error variance (unit is K^2).

2.5 Conclusion

This study has shown that the Kalman filter can be considered as a very good tool when it is implemented with a rather simple model. It improves knowledge of the statistical error structures (and their time evolution) which is a prerequisite for a sophisticated objective analysis scheme.

Unfortunately, the high costs of the Kalman filter will most likely prevent its use in the near future. However, some experiments are currently carried out to investigate if such a scheme could be used with a coarse resolution to model the error covariance time evolution.

3 DIFFICULTIES TO IMPLEMENT A VARIATIONAL ANALYSIS

3.1 Introduction

In a recent paper, Jarraud and Geleyn (1988) presented the strategy of the French DMN for numerical weather studies. As France is a member state of ECMWF, it has been decided to focus the internal research and operational efforts in numerical weather prediction on the short range (from 0 to 72 hours). The current operational system has revealed some deficiencies and limitations. This has led to the definition of an ambitious new project based on a variable mesh spectral model with a more consistent processing of water cycle and on

a variational analysis, initially three dimensional and later four dimensional.

Jarraud and Geleyn (1988) quote Talagrand and Courtier (1987) who have proposed to use a variational method to cure (or at least alleviate) some of the known deficiencies of the optimum interpolation. Some of the benefits expected are, for instance:

(i) removal of sophisticated data selection algorithms;
(ii) absence of discontinuities in the analysed fields;
(iii) better use of new kinds of data;
(iv) better integration of constraints (e.g. geostrophism);
(v) ability to include initialization in the analysis.

3.2 Presentation of the problem

The variational method consists in minimizing a cost function by using an iterative scheme which requires the computation of the cost function and its gradient (see Courtier, 1987). In the close future, a four dimensional variational analysis seems far too expensive to be operationally implementable. Both the necessary computing time and the required storage allocation cannot be supplied by current computers.

However, a three dimensional variational analysis deserves to be studied, because some advantages of the method,

such as those listed in section 3.1, could lead to an improvement of the analysis quality. Three dimensional analysis means that the variable time is not taken into account, i.e. the cost function is not time dependent.

The scalar cost function J is a function of the atmospheric state vector X, i.e. X is the variable to be analysed. The function J can be defined as the sum of three contributions :

$$J(X) = J_{obs}(X) + J_{pre}(X) + J_{con}(X)$$

where J_{obs} is a function of the "distance" between the atmospheric state X and the observations, J_{pre} is a function of the "distance" between X and the state corresponding to a guess-field usually provided by a numerical prediction model, J_{con} is representative of some constraints which are supposed to be valid for the final solution. As some problems with J_{obs} and J_{pre} still await a solution, it is still too early to study the contribution J_{con}.

According to Jazwinski (1970), it is possible to define a cost function J to get an equivalence with the statistical optimum interpolation if the link operator H (between the observations and the guess field) is linear. In such conditions, J is decomposed as follows :

$$J_{obs}(X) = {}^t(H.X-R).O^{-1}.(H.X-R)$$
$$J_{pre}(X) = {}^t(X-Xg).P^{-1}.(X-Xg)$$

where Xg is the guess field atmospheric state, H is the link operator between X and the observations, P is the guess field error covariance matrix and O is the observation error covariance matrix. The letter t denotes the transposition for a vector.

It is a prerequisite to test the feasibility of the method since several problems must be faced : central memory and computing time requirements, efficiency of the iterative scheme, independence of the results on initial conditions, final result quality... A definitive answer must be given by the beginning of 1989 and the definition phase will then start.

3.3 Consequences of the use of observations

3.3.1 Data checking

It is obvious that all the observed data must be carefully checked before use. The optimum interpolation is a useful tool for this purpose, since an analysed value can be easily estimated at each observation location without using the observation to be checked. Then a comparison between the analysed value and the observed value allows a choice : either keep a good data or discard a wrong data.

Such a scheme cannot be simply implemented in the variational analysis, as any analysed value is obtained as a result of a heavy iterative scheme. Moreover, as an iterative scheme is used, it is important to decide whether a value is either good or wrong. Otherwise, if an observation is good for some descent steps and wrong for other steps, the scheme could not converge. Anyway, even if it is desirable to perform the data checking in the variational analysis, a solution must be found for two problems: (i) how to validate an observation without using the observation itself; (ii) how to evaluate the quality of a variational analysis. The computation of the second derivation of the cost function brings information on the analysis quality, but this seems to be rather expensive.

Therefore, a preliminary optimum interpolation analysis seems necessary to check the data before the variational analysis. This would be the least expensive way to provide the variational scheme with clean data.

3.3.2 Observation error statistics

The implementation of an analysis scheme requires the knowledge of observation error statistics for all the observing systems. The "observation error" can be split into two parts. First there is the instrumental error, which is generally not correlated with other measurements performed by other instruments. Correlations are however significant when the same instrument makes several measurements (ascending balloons TEMP, SATEM, SATOB...).

Then there is the representivity error. The observed parameter can be different from the parameters which can directly be forecast. Therefore a link operator is necessary between both parameters for converting their values, but this link operator cannot be perfect which implies modelling errors. Besides, the observed data correspond to certain scales of time and space whereas the forecast model has other time and space characteristics. All the phenomena with small scale characteristics cannot be represented by the forecast model, and this induces other representivity errors. Of course, the two sources of representivity errors involve significative correlation values between observations.

If the forecast model has a variable mesh, the variance of the representivity error will change from one location to another (even for the same observing system), and neighbour observations will be highly correlated. As a consequence, the variable variances and the associated correlations must be modelled. They will vary with respect to both the observing systems and the geographical location. Moreover, the complete observing error covariance matrix used in J_{obs} will not be as hollow as expected. Its handling will require more computing time and more memory allocation.

3.4 Distance with respect to the first-guess

3.4.1 Study of the matrix P

As shown in section 3.2, the contribution J_{pre} implies some handling of the matrix of prediction error covariances P. This is the major difficulty with the variational analysis since such a matrix is quite huge. Its dimension is equal to the number of degrees of freedom of the prediction model.

Instead of working on a covariance matrix, it is better to look after the associated correlation matrix and to normalize the differences between the first-guess field and the unknown field. This is a good means to use geographically variable prediction error variances, since they will be included in the normalization coefficients.

In the current situation, correlations are computed in the physical space with a model based either on gaussian functions or Bessel function or other functions. Such a matrix P is symmetric and its terms far from the diagonal decrease and can be neglected. For a one level spectral model with a triangular truncation Tm and v variables, the dimension of P in the physical space is: dim = (3m+1).(3m+1).v.

Therefore, its total size is dim*dim. In the spectral space, the dimension of P is only (m+1).(m+2).v. Consequently, it seems interesting to stick to the spectral space to cope with the matrix P. Moreover, it has been demonstrated that if

the error correlations are isotropic and homogeneous, the matrix P is diagonal (Courtier, 1987). Correlations may vary a little with the location, but even though it is expected that P will remain easy to handle. As such variations of the correlations are usually implemented, a study was carried out on the shape of the matrix P and the consequences of some simplifications.

Although such a study is rather simple from a theoretical point of view, its practical implementation needs a large memory storage allocation. With skilful programming, the requested space is about $3m^4$ words if m is the truncation. For instance, the total size needed with a one level one variable T79 model is about 117 millions words.

The provisional results are as follows. As soon as the correlations vary with the location, the matrix P is not diagonal in the spectral space. If the matrix P is then modified to be diagonal in the spectral space (only the diagonal values are kept), the corresponding matrix P in the physical space is rather different from the initial one.

Another way was explored, following the works of Phillips (1986) and Parrish (1988). If some of their assumptions are correct, the matrix P must be diagonal in the normal modes space associated with the prediction model. This was experimentally checked. Unfortunately, as soon as the correlations are not homogeneous, the matrix P is not diagonal again.

In order to conclude, it is obvious that the size of the matrix P will be an important problem to be solved. If some very stringent assumptions must be proposed to make the matrix P diagonal, this is not satisfactory because the optimum interpolation would be a better scheme. As the normal mode space is not very user-friendly, a special effort will be taken to carry on the investigations in the spectral space.

3.4.2 Convergence of the iterative scheme

A small simple experiment was carried out to check the convergence of the iterative scheme. A simulated one level variational analysis of a geopotential height field was designed on a 15 x 15 grid with a guess field, sixty observations, constant prediction error variances, constant observation error variances, gaussian correlation with inflexion at 500 km, mesh size of 300 km. The cost function is the one proposed in section 3.2. The iterative scheme requires several ingredients: evaluation of the cost function, evaluation of its gradient and definition of a scalar product.

When the scalar product is the classical Euclidian scalar product, i.e. $(X,Y) = {}^{t}X.Y$, the method does not converge. The trouble comes from the contribution J_{pre}. This is due to the fact that the correlation matrix P (size 225 x 225) is rather unstable. Its determinant is about 10^{-500}. The evaluations of the cost function and its gradient are not very

stable either since they use the inverse of P. Under such conditions, the scheme is not satisfactory.

Another scalar product can be chosen to improve the conditionment of the problem. For instance, if the scalar product is $(X,Y) = {}^{t}X.P^{-1}.Y$, the method does converge. One drawback is that the evaluation of the gradient for Jobs is more difficult.

As a conclusion, this short experiment shows an important sensibility of the method with the ingredients to the iterative scheme. The problem must become more difficult when the size of P increases because its determinant will be equal to zero for the computer. Hence some clever algorithms will have to be found to handle the inverse of P.

3.5 Provisional conclusion

It seems still too early to draw definitive conclusions about the feasibility of a three dimensional operational variational analysis for the beginning of the 1990's. The main problems are identified: lack of quick efficient data checking inside the variational method, possible difficulties to rapidly converge with the iterative scheme, difficulties of memory storage for all the necessary ingredients associated with the guess-field handling and difficulties to limit the required computing time to reach a result.

A preliminary optimum interpolation analysis should be indispensible in order to check all the observed data before use and to give the iterative scheme initial fields close to the final solution. The principal items to be studied for the next months are: (i) to carry on the work on the contribution J_{pre} (first with a 2D scheme, then with a 3D scheme), (ii) to deal with the highly correlated observations such as SATEMs or SATOBs, (iii) to investigate efficient algorithms for rapid convergence of iterative schemes, (iv) to study error structure functions with respect to a variable mesh prediction model.

4 VARIATIONAL INVERSION OF RAW RADIANCES

4.1 Introduction

The use of data which are non-linearly related to the analysis parameters is a crucial problem for operational assimilation schemes. For instance, optimal interpolation used in most operational centres does not permit a simple use of this kind of data.

In contrast, variational methods offer a powerful way of solving this kind of problems through a more or less simple minimization process. The coding of the adjoint of the associated operator is the major practical difficulty for the implementation of the method.

As satellite radiances are to become a major source of information for weather prediction, it is important to set up efficient methods to deal with them. The goal of the study is to retrieve a vertical temperature and humidity profile using a first guess profile and a set of observed HIRS radiances. The link operator is the radiative transfer equation, which can be modelled with the "TOVS Export Package" released by the University of Wisconsin.

4.2 Theory and implementation

Variational methods have been suggested for a long time in meteorological science. Here, the variational method consists in minimizing a cost function by using an iterative method which requires the computation of the cost function and its gradient at each minimization step.

The scalar cost function J is defined as the sum of two contributions: the first one estimates the distance between the unknown profile and the first guess-field whereas the second one estimates the distance between the unknown profile and the observed raw radiances. The retrieved profile solution is the one which minimizes the complete function J.

The corresponding mathematical equation can be written as:

$$J(X) = {}^{t}(X-Xg).P^{-1}.(X-Xg) + {}^{t}(H.X-R).O^{-1}.(H.X-R)$$

where X is the analysis variable (i.e. an unknown vector containing a temperature and humidity profile), Xg is the first guess profile, R is the vector corresponding to an observed HIRS radiance data set, H is the radiative transfer model (inputs = temperature and humidity profiles; output = synthetic radiances), P is the guess field error covariance matrix and O is the observation error covariance matrix.

The gradient of J with respect to X is estimated by:

$$\nabla_x J(X) = 2.P^{-1}.(X-Xg) + 2.\tilde{H}^{*}.O^{-1}.(H.X-R)$$

where $\tilde{H}^{*}$ is the adjoint of the linear tangent model associated with the radiative transfer model H. Should H have been linear, the optimum interpolation would have been powerful enough to solve the problem, as shown by Jazwinski, 1970.

Nevertheless, some difficulties must be removed before implementing the method. As the radiative transfer model is rather sophisticated, the adjoint model cannot be analytically derived. Therefore, the adjoint model was directly encoded in Fortran from the linearized direct model, i.e. the program TOVSRAD (extracted from the TOVS Export Package) after linearization. A problem could have occured to the relative

humidity processing since the variable cannot be differentiated in the vicinity of its thresholds. Fortunately, this difficulty was overcome because all the processed values were far enough from these thresholds.

The matrices P and O where chosen as a blend of the ones used by Eyre (1987) and the French meso-scale PERIDOT model statistics. The conjugate gradient method then becomes an efficient tool for the minimization process: a solution for a retrieved atmospheric profile can be reached.

Before using the minimization scheme, it is important to check the direct model linearity (the model should better be rather linear). This was performed close to various equilibrium states. The results were globally satisfactory, although the water vapour absorption channels were found rather non linear. This is due to the transmittance high dependency with respect to the water content for these channels. As a consequence, a particular attention must be paid to the HIRS channel 11 and mostly channel 12. Moreover, the cost function must have only one local minimum in order to help the minimization scheme. This was successfully tested by checking various projections of the cost function.

4.3 Results

In order to retrieve atmospheric profiles from raw radiances, the following experiments were set up. "True"

profiles were chosen from numerical prediction model outputs. Then, corresponding synthetic radiances were computed with the radiative transfer equation model. These radiances were evaluated as clear "true" radiances. These radiances are then modified by small perturbations compatible with the given observational error covariance matrix. The "true" profiles are similarly modified by perturbations consistant with the prediction error covariance matrix. The obtained profiles can be used both for providing relevant information and for initializing the minimization process.

The first result is the feasibility of the method. A minimum is found for each radiance set and it corresponds to a meteorologically relevant atmospheric profile. This was reached after a few iterations, generally less than ten steps. The upper levels converge more rapidly, probably because the information is more independent in the stratospheric levels. On the other hand, the method converges a bit slower in the planetary boundary layer due to the information redundancy.

A great deal of experiments were carried out to check the quality of the retrieved profiles. To avoid saturation problems, the "true" profiles were perturbed only with temperature modifications. This is a limitation because the humidity first guess profiles are considered perfect, but this has a weak impact on the temperature retrieval. Besides, the first guess profiles were used to initialize the minimization scheme.

FIRST GUESS FIELD ERROR STANDARD DEVIATION			OBSERVATION ERROR STANDARD DEVIATION		
Level (hPa)	Temperature (degrees)	Humidity (g/kg)	Channel	Error correlated (degrees)	uncorrelated (degrees)
44	2.01	1.65	1	0.55	4.00
100	1.90	1.65	2	1.00	0.55
150	1.72	1.65	3	1.05	0.45
200	1.99	1.65	4	0.45	0.45
250	2.69	1.65	5	0.70	0.30
300	1.90	1.72	6	0.80	0.60
400	2.03	1.80	7	1.00	1.00
500	1.75	1.70	8	1.40	2.00
600	1.87	1.65	9	6.00	20.00
700	1.90	1.59	10	1.40	1.50
800	2.06	1.51	11	3.50	1.50
850	2.15	1.45	12	3.50	1.80
900	2.32	1.42	13	1.25	0.75
950	2.50	1.38	14	1.10	0.50
1000	2.53	1.35	15	0.70	0.20
Tsol	3.67		16	9.90	1.00
			17	2.05	0.15
			18	1.40	2.20
			19	1.40	2.20

Table 1 : first guess field error standard deviation and observation error standard deviation with and without spatial correlation.

Table 1 displays the r.m.s. of observation errors and first guess errors. The temperature first guess error r.m.s. is about 2 K. After retrieval, this temperature r.m.s. is about 1 K, as seen on figure 12. This result is consistant with the one of Eyre (1987) in spite of different circumstances. The humidity error r.m.s. corresponds to the temperature impact on the humidity via the water channels and the first guess cross correlation between temperature and humidity.

4.4 Conclusion

The experiments carried out up to now have demonstrated the feasibility of the method with clear radiances. The error r.m.s. related to the retrieved temperature and humidity fields are very encouraging. Similar experiments are under way with cloudy radiances. Extensions can be envisaged with three dimensional (and even four dimensional) retrieval.

5 IMPACT STUDY OF SATELLITE DATA IN A MESO-SCALE SCHEME

5.1 Presentation of the experiment

This study was carried out in order to achieve two goals. Firstly, the satellite data impact must be assessed for a meso-scale assimilation system ; secondly, various methods

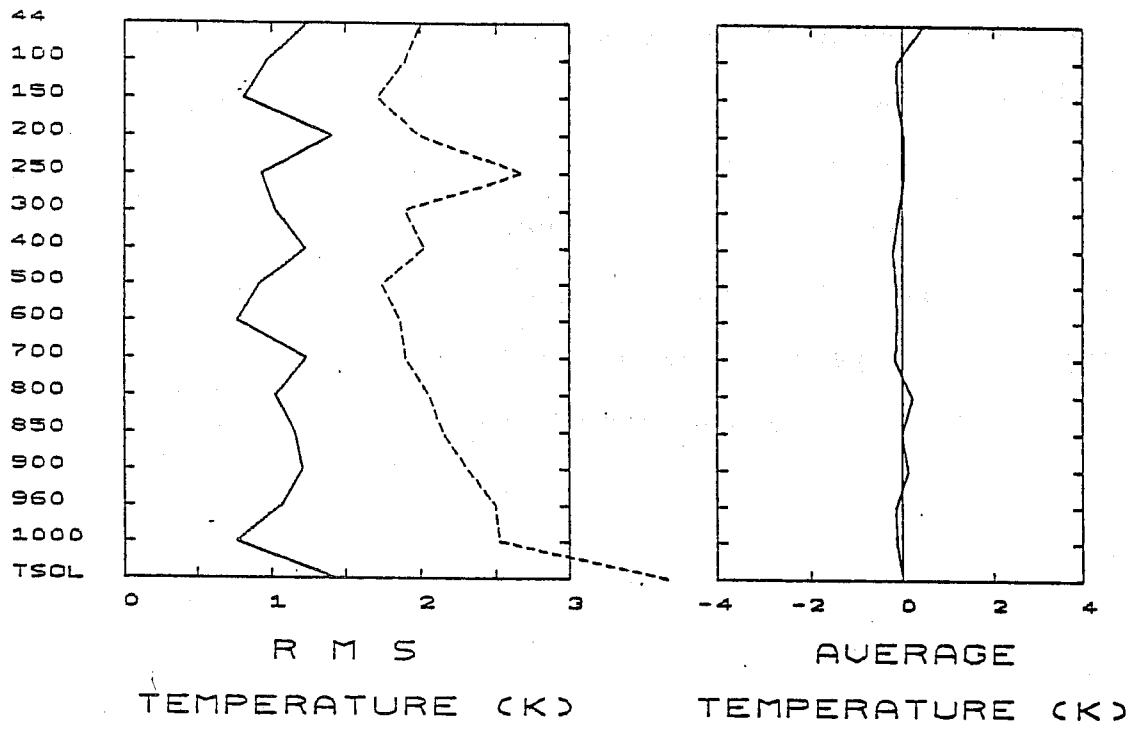

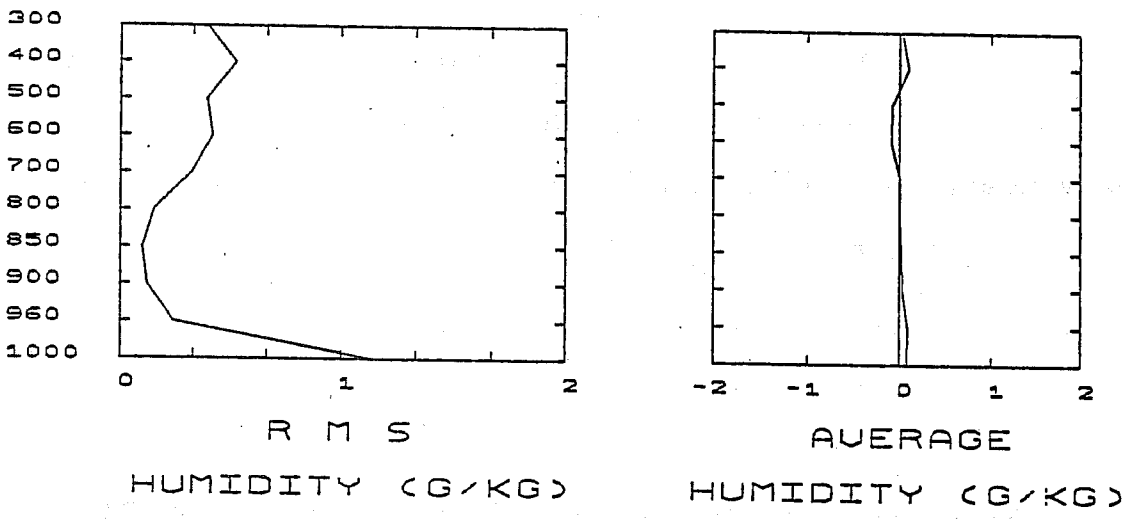

Figure 12 : r.m.s. of errors and bias. —— background errors
---- retrieval errors

for inserting satellite observation in a meso-scale objective analysis scheme must be compared.

The assimilation system used is the current French operational PERIDOT system. Its main characteristics are described below.

Analysis

The objective analysis is performed by a multi-variate three dimensional optimal interpolation for the prognostic variables of the model (Surface Pressure, Temperature and Wind Components) on the prediction model's sigma levels, followed by a relative humidity analysis on slabs related to model layers. This is described in the paper of Durand and Bougeault (1987). The data which can be assimilated are the GTS data and the raw radiances (clear and partly cloudy HIRS and MSU data). These radiances can be directly used by the scheme without any retrieval.

Forecast model

Predictions are obtained by a grid point sigma coordinate primitive equation model (C grid). The domain is a stereographic 95 x 95 square grid centered over western Europe with a mean mesh of about 35 km. The vertical sigma grid consists of 15 levels, with a parabolic dependency towards the bottom. The temporal discretization uses a leap-frog semi-implicit scheme with a 4 minute time step. A

complete description is given in the publication of Imbard et al. (1987).

Several parallel runs were performed. The assimilation step was set to 6 hours. The lateral boundary conditions were provided by the ECMWF operational analyses; they are identical for all the assimilation runs. Therefore the observed impact will only involve the satellite data over the PERIDOT domain.

The assimilation period starts from 30 January 1987 at 0 UTC and ends at 12 UTC on 3 February 1987. This time interval was chosen for four reasons :

(i) two polar orbiting satellites were in nominal operation;
(ii) corresponding magnetic tapes with high resolution satellite data were supplied by NOAA/NESDIS to ECMWF;
(iii) ECMWF has applied the LMD "3I programme" on the NOAA/NESDIS data to get other retrieved profiles (see Chedin et al. (1985));
(iv) other experiments, with various domains and resolutions, were carried out over the same period by other centres (ECMWF, UKMO, HIRLAM).

5.2 Description of the data sets

Six data sets were used as input for six assimilation runs. Each run is called by an upper case letter.

* The run "A" is the reference run. All the land based observations are used, including upper air messages TEMP's, PILOT's and AIREP's. There is no satellite data.

* The run "S" includes all the data of "A" and the operational SATEM's with 500 km resolution. These SATEM's were produced by NOAA/NESDIS with the TOVS package.

* The run "T" includes all the data of "A" and the SATEM's with 250 km resolution produced by NOAA/NESDIS. These SATEM's are called TOVS at ECMWF.

* The run "N" includes all the data of "A" and high resolution SATEM's (80 km) produced by NOAA/NESDIS.

* The run "R" includes all the data of "A" and clear radiances data. In practice, about 40 % of these radiance data have information only for stratospheric HIRS channels (channels 1, 2, 3 and 17), because the other channels were too much polluted by clouds. This is a major difference to the daily operational runs at the DMN.

* The run "I" includes all the data of "A" and temperature profiles retrieved by the "3I method". Only partial results are now available for this run.

5.3 Main results

5.3.1 Differences between analyses

Differences between analyses were evaluated for all the assimilation steps. Tables 2 to 4 give r.m.s. of the analyses differences "S"-"A", "T"-"A", "N"-"A" and "R"-"A". Moreover, charts of differences (see figures 13 to 16) are displayed and show a slight impact of the satellite data.

Date	"S"-"A"	"T"-"A"	"N"-"A"	"R"-"A"
30 Jan 00	.11	.36	.52	.32
30 Jan 06	.59	1.12	1.17	.71
30 Jan 12	.52	.89	1.21	.65
30 Jan 18	.85	1.52	1.60	1.00
31 Jan 00	.36	.73	1.27	.63
31 Jan 06	.66	1.51	1.64	.86
31 Jan 12	.45	.97	1.30	.69
31 Jan 18	.65	1.32	1.60	.84
01 Feb 00	.39	.68	1.20	.53
01 Feb 06	.63	1.22	1.00	.52
01 Feb 12	.70	1.03	1.12	.67
01 Feb 18	.62	1.35	1.27	.92
02 Feb 00	.40	.58	.95	.70
02 Feb 06	.68	1.26	1.15	1.16
02 Feb 12	.45	.84	.98	.76
02 Feb 18	.52	1.34	1.13	1.09
03 Feb 00	.33	.51	.62	.64
03 Feb 06	.49	1.05	.96	.78
03 Feb 12	.35	.62	.84	.47
Average	.51	.99	1.13	.73

Table 2: Difference rms between temperature analyses at sigma level 3 (about 300 hPa). Unit: Kelvin

This impact increases with the finest space resolution of SATEM data ("S"-"A" "T"-"A" "N"-"A"). The results seem less significant with the radiances, but this can be explained by the great deal of incomplete radiance sets and the absence of

partly cloudy radiances (which the PERIDOT analysis usually assimilates).

Date	"S"-"A"	"T"-"A"	"N"-"A"	"R"-"A"
30 Jan 00	.08	.15	.22	.19
30 Jan 06	.31	.47	.55	.42
30 Jan 12	.24	.39	.44	.36
30 Jan 18	.33	.59	.64	.46
31 Jan 00	.22	.41	.39	.29
31 Jan 06	.29	.62	.63	.47
31 Jan 12	.22	.44	.52	.40
31 Jan 18	.32	.57	.62	.47
01 Feb 00	.17	.31	.40	.33
01 Feb 06	.24	.42	.44	.42
01 Feb 12	.32	.52	.53	.40
01 Feb 18	.33	.50	.67	.59
02 Feb 00	.23	.37	.42	.53
02 Feb 06	.24	.44	.55	.70
02 Feb 12	.21	.39	.50	.67
02 Feb 18	.31	.54	.65	.66
03 Feb 00	.25	.45	.42	.33
03 Feb 06	.28	.56	.64	.45
03 Feb 12	.30	.36	.45	.28
Average	.26	.45	.51	.44

Table 3: Difference rms between temperature analyses at sigma level 5 (about 500 hPa). Unit: Kelvin

However, charts of differences show a good consistency between direct use of radiance and use of SATEM data: same impact location, same variation sign. The problem still remains to find out whether this impact is either positive or negative.

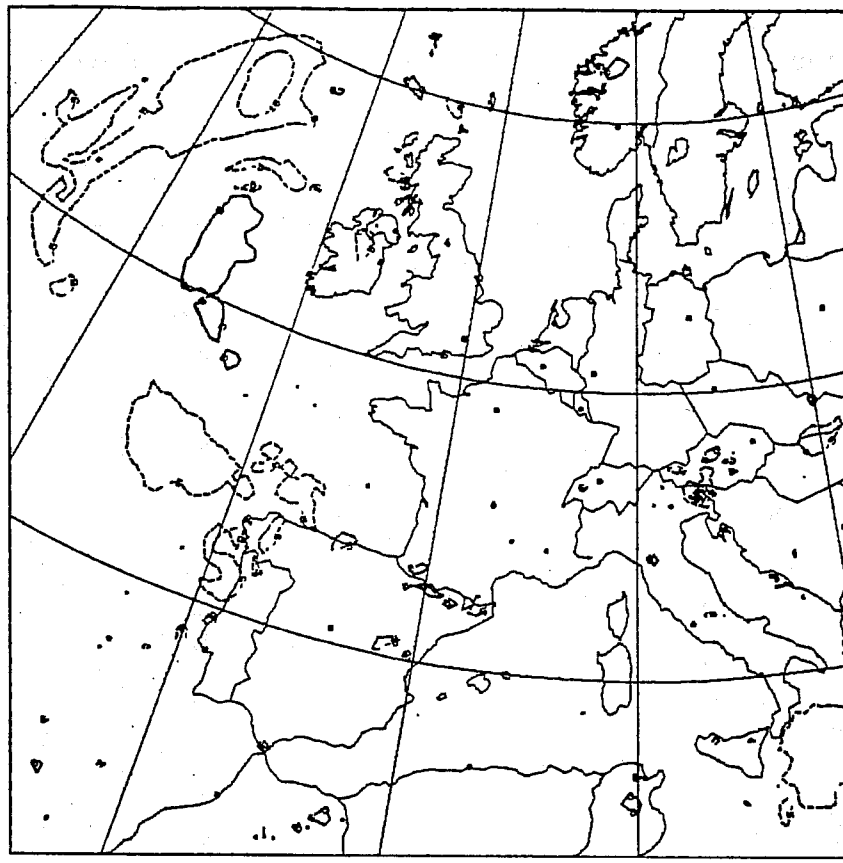

Figure 13 : - differences between temperature analyses "S" and "A" at 850 hPa for 02/02/87 at 0 UTC, in 1/10 K, plotting interval 1 K.

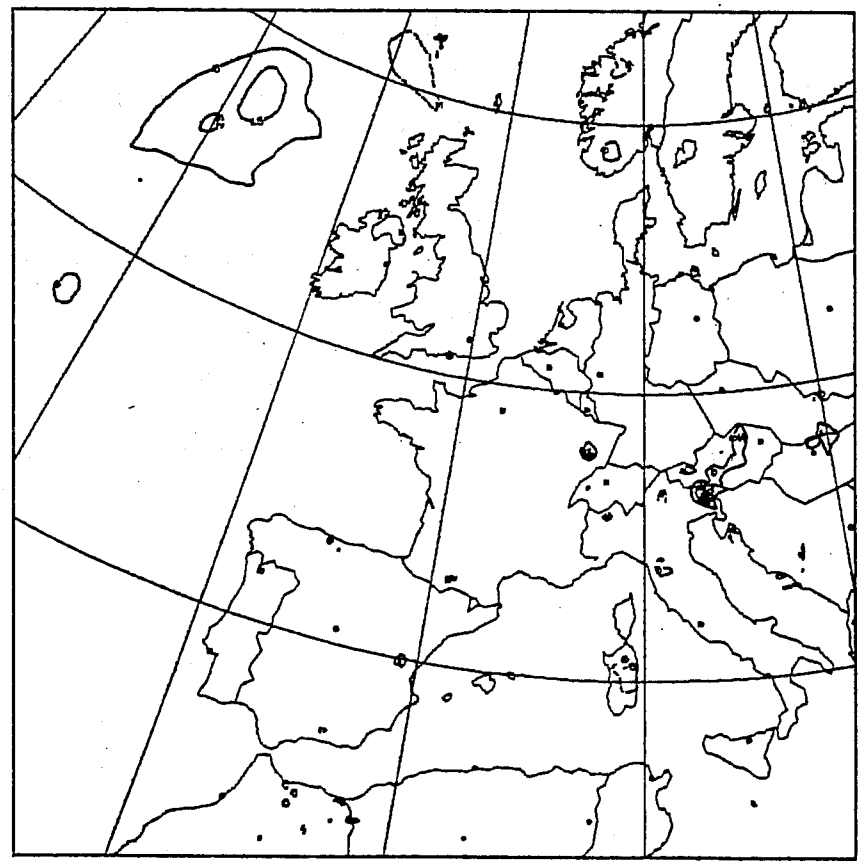

- same as above, for sea level pressure differences in 1/10 hPa, plotting interval 1 hPa.

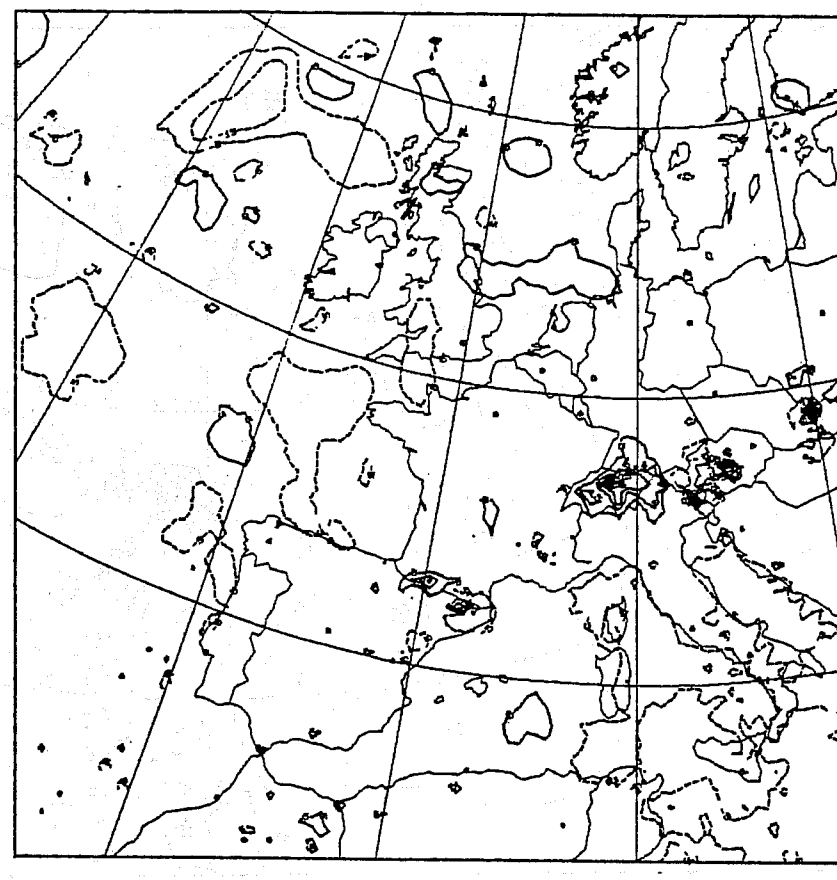

Figure 14 : - differences between temperature analyses "T" and "A" at 850 hPa for 02/02/87 at 0 UTC, in 1/10 K, plotting interval 1 K.

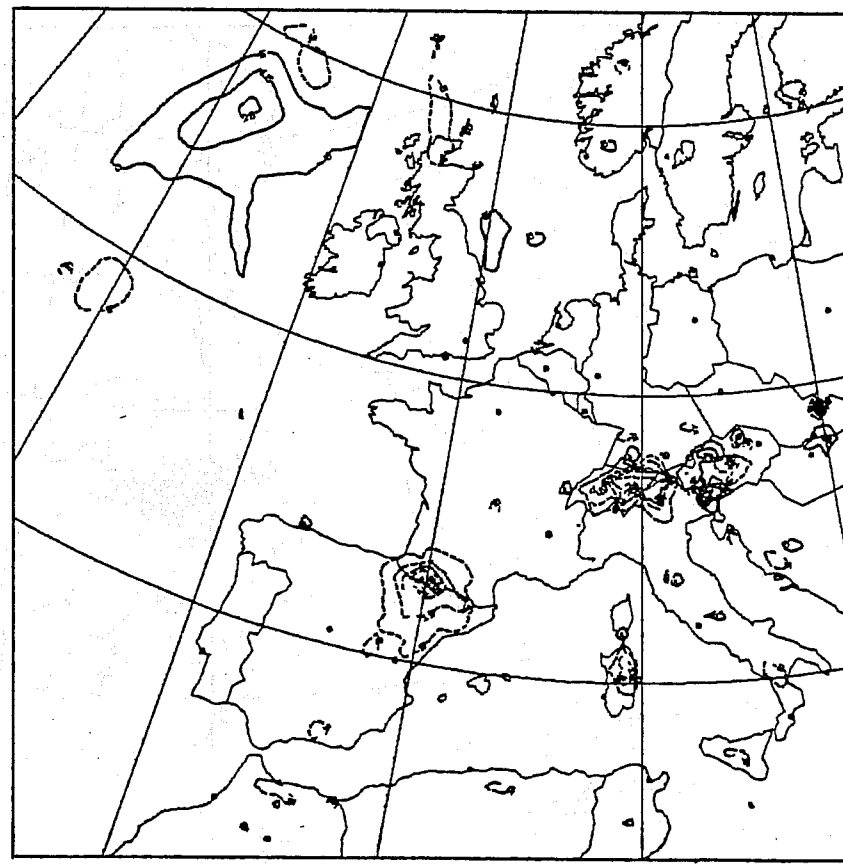

- same as above, for sea level pressure differences in 1/10 hPa, plotting interval 1 hPa.

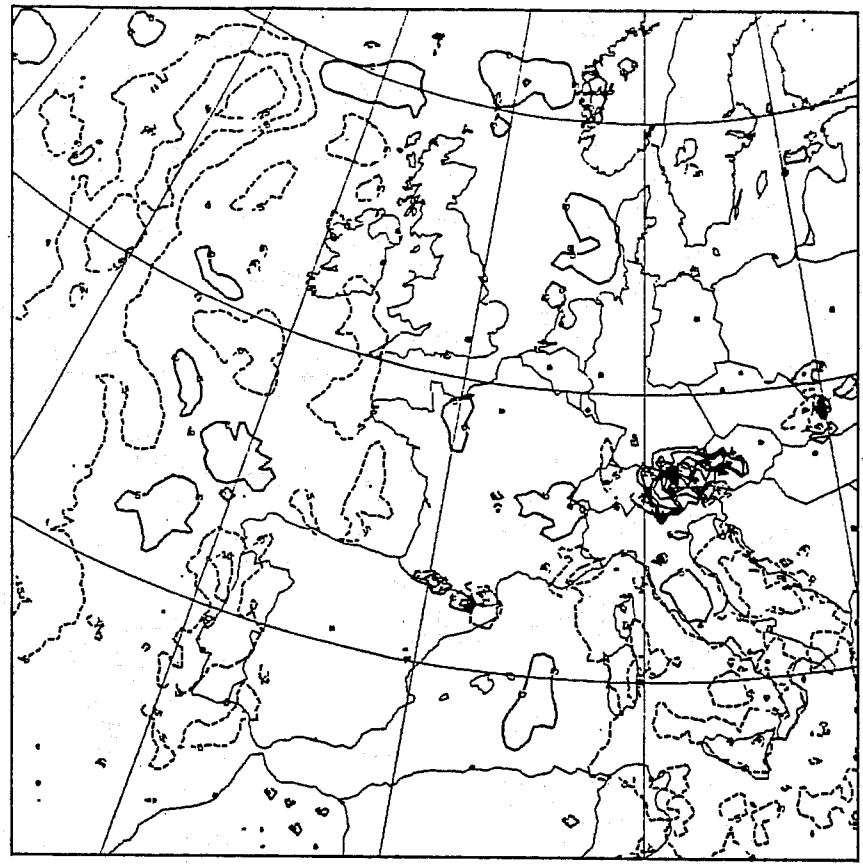

Figure 15 : - differences between temperature analyses "N" and "A" at 850 hPa for 02/02/87 at 0 UTC, in 1/10 K, plotting interval 1 K.

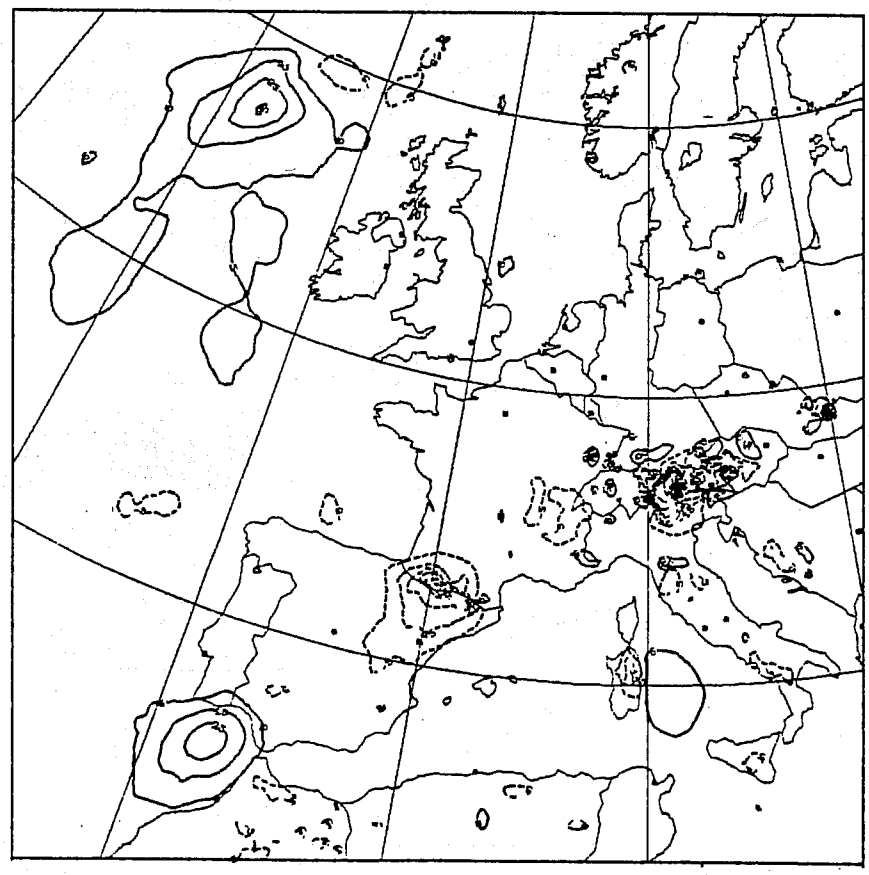

- same as above, for sea level pressure differences in 1/10 hPa, plotting interval 1 hPa.

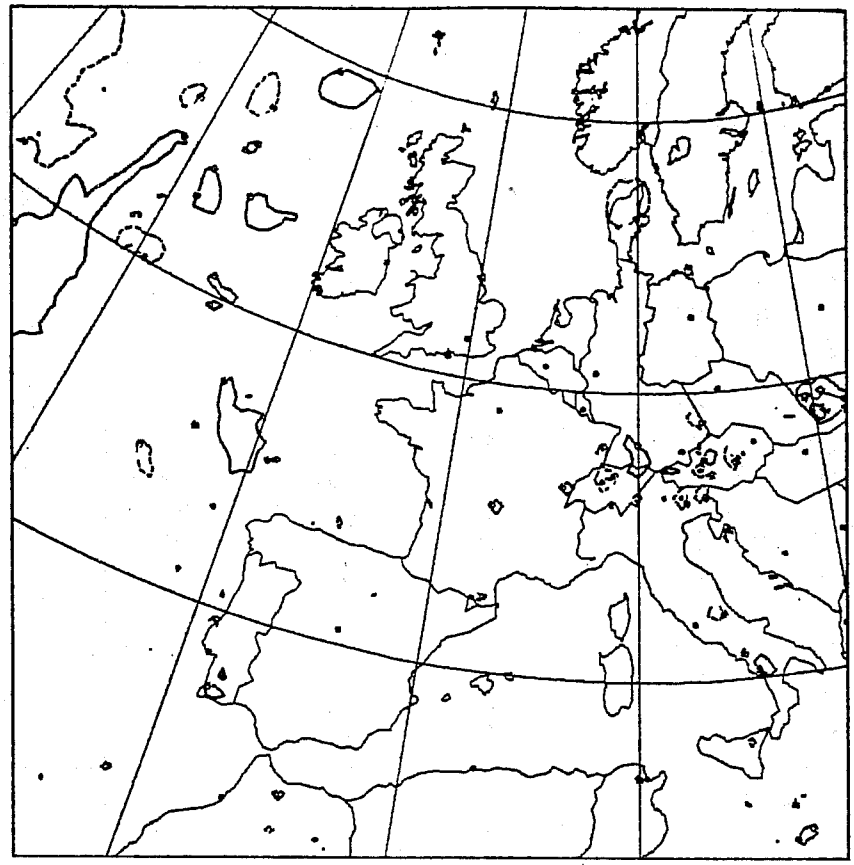

Figure 16 : - differences between temperature analyses "R" and "A" at 850 hPa for 02/02/87 at 0 UTC, in 1/10 K, plotting interval 1 K.

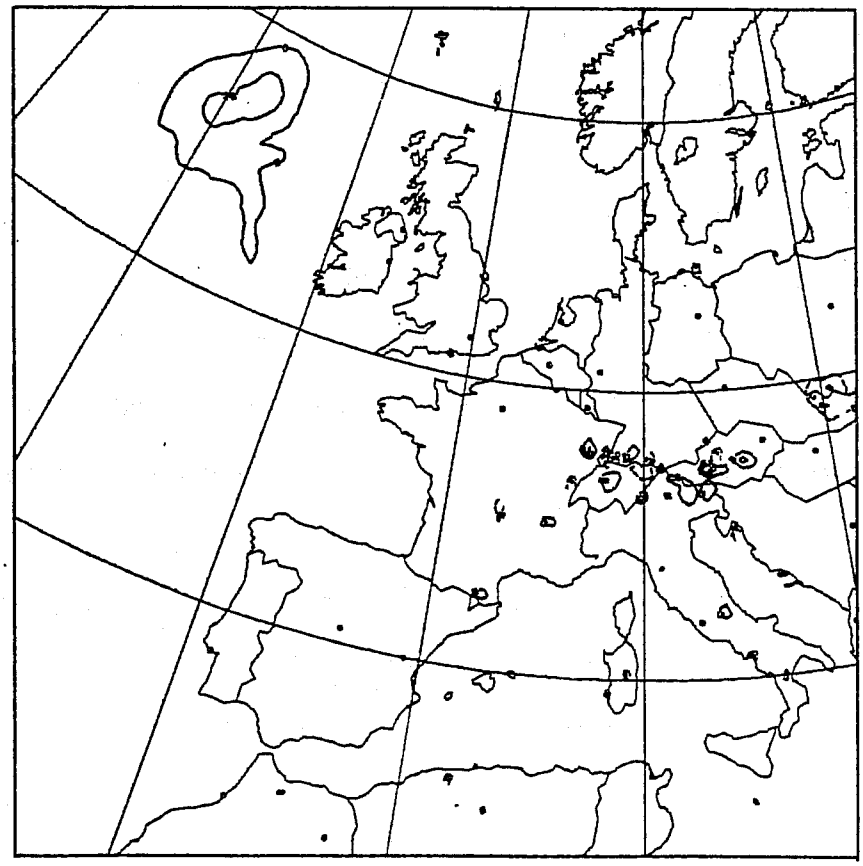

- same as above, for sea level pressure differences in 1/10 hPa, plotting interval 1 hPa.

Date	"S"-"A"	"T"-"A"	"N"-"A"	"R"-"A"
30 Jan 00	.05	.10	.20	.06
30 Jan 06	.26	.37	.65	.31
30 Jan 12	.23	.35	.60	.27
30 Jan 18	.27	.50	.61	.29
31 Jan 00	.19	.30	.41	.21
31 Jan 06	.22	.48	.59	.32
31 Jan 12	.17	.35	.52	.30
31 Jan 18	.25	.37	.63	.27
01 Feb 00	.26	.48	.59	.35
01 Feb 06	.32	.53	.64	.46
01 Feb 12	.42	.52	.58	.29
01 Feb 18	.36	.50	.72	.27
02 Feb 00	.30	.46	.60	.36
02 Feb 06	.38	.54	.75	.38
02 Feb 12	.23	.37	.58	.34
02 Feb 18	.34	.44	.67	.37
03 Feb 00	.39	.48	.55	.36
03 Feb 06	.38	.51	.75	.45
03 Feb 12	.28	.31	.52	.37
Average	.28	.42	.59	.32

Table 4: Difference rms between temperature analyses at sigma level 15 (about 15 m). Unit: Kelvin

5.3.2 Comparison between guess-fields and observations

The guess-fields are 6 hour forecast fields computed by the PERIDOT prediction model. The quality of the assimilation scheme can be evaluated by comparing the guess-fields with the radiosondes (for upper levels) and surface observations. These observations are the core of the reference run "A", but they are mostly available above land, i.e. about half of the domain. Statistics displayed in tables 5 and 6 generally show no degradation above land, but a doubt remains for the run "N" corresponding to 80 km SATEM's.

Date	"A"	"S"	"T"	"N"	"R"	Nb.obs.
30 Jan 00	13.10	13.10	13.10	13.10	13.10	67
30 Jan 12	13.70	13.50	14.00	13.60	13.40	75
31 Jan 00	16.40	15.90	15.70	14.80	16.20	69
31 Jan 12	16.90	16.30	16.30	16.20	16.90	75
01 Feb 00	12.90	12.50	12.20	12.50	13.70	68
01 Feb 12	12.70	12.40	12.50	12.90	12.90	72
02 Feb 00	11.70	11.10	11.20	11.90	11.60	65
02 Feb 12	18.40	17.70	17.30	18.20	17.80	72
03 Feb 00	17.10	16.10	15.90	15.60	16.60	66
03 Feb 12	10.60	10.60	10.20	10.90	10.60	69
Average	14.49	14.01	13.92	14.07	14.41	
rms	2.76	2.55	2.51	2.33	2.55	

Table 5: Statistics on the difference rms "guess-field minus observation" at 500 hPa level. Unit: Meter.

	"A"	"S"	"T"	"N"	"R"	Nb. obs. (*)
30 Jan 00	9.64	9.64	9.64	9.64	9.64	799
30 Jan 06	11.85	11.82	11.78	11.66	11.81	1061
30 Jan 12	14.13	14.05	13.87	14.01	14.05	1088
30 Jan 18	11.27	10.97	11.00	11.04	11.22	1056
31 Jan 00	9.83	10.02	10.20	10.51	9.94	807
31 Jan 06	11.56	11.42	11.41	11.42	11.53	1041
31 Jan 12	11.16	11.41	11.72	11.89	11.28	1045
31 Jan 18	10.08	10.11	10.19	10.12	10.07	1021
01 Feb 00	10.57	10.46	10.54	10.69	10.39	818
01 Feb 06	10.85	10.79	11.10	11.15	11.00	1033
01 Feb 12	11.55	11.48	12.41	11.90	11.45	1078
01 Feb 18	11.77	12.04	12.01	11.92	11.68	1038
02 Feb 00	10.79	10.87	11.12	11.30	11.04	795
02 Feb 06	11.93	12.17	11.97	11.84	11.78	1074
02 Feb 12	10.84	11.17	10.80	11.24	11.12	1131
02 Feb 18	11.43	11.36	11.51	11.72	11.66	1052
03 Feb 00	10.37	10.53	10.75	10.43	10.53	791
03 Feb 06	10.98	10.81	10.59	10.81	10.93	816
03 Feb 12	11.38	11.56	11.56	11.42	11.17	1100
Average	11.24	11.28	11.36	11.39	11.26	
rms	.94	.92	.89	.85	.89	

Table 6: Statistics on the difference rms "guess-field minus observation" at surface level. Unit: Meter.
(*) This is the number of observations used for run "A"

5.3.3 Quality of forecast fields

The forecast experiments are presently being carried out. Only a few results are available. A paper must be devoted to this impact study and all the results are supposed to be submitted as soon as the study will end.

6 CONCLUSION

Four independent studies were presented and concluding remarks were given. At this point, an overall conclusion will be drawn.

Some promising results were already obtained with variational methods. The processing of raw radiances is a good example. The implementation of a variational scheme still seems difficult for an operational exploitation. Many problems must be solved before the present feasibility study can be concluded.

As a consequence, the present studies must be continued. It is however expected that the future improvements in computer (hardware and software) will bring an important help for developing variational methods, since huge central memory and computing time will be needed.

REFERENCES

Chedin, A., N.A. Scott, C. Wahich and P. Moulinier, 1985: The Improved Initialization Inversion method: a high resolution physical method for temperature retrievals from the Tiros-N series. J. Clim. Appl. Met., 24, 124-143.

Cohn, S. and D. Parrish, 1985: A Kalman filter for a two dimensional shallow water model: formulation and preliminary experiment. NMC Office Note No 304, Washington DC 20233.

Courtier, Ph., 1987: Application du contrôle optimal à la prévision numérique en météorologie. Thèse de doctorat de l'université de Paris 6.

Durand, Y. and Ph. Bougeault, 1987: L'analyse objective Péridot. DMN/EERM technical note No 193, 71pp.

Eyre, J.R., 1987: Inversion of cloudy satellite sounding radiance by non linear optimal estimations: theory and simulations for TOVS. Submitted to Q.J.R.M.S.

Ghil, M., S. Cohn, J. Tavantzis, K. Bube and E. Isaacson, 1980: Application of estimation theory to numerical weather prediction. ECMWF workshop report, 249-333.

Imbard, M., A. Craplet, Ph. Degardin, Y. Durand, A. Joly, N. Marie and J.F. Geleyn, 1987: Fine mesh limited area forecasting with the french operational "Péridot" system. ECMWF seminar.

Jarraud, M. and J.F. Geleyn, 1988: Current plans for short range NWP at DMN: the Arpège Project. Eighth conference on numerical weather prediction, Baltimore, Md. AMS, Boston.

Jazwinski, A.H., 1970: Stochastic processes and filtering theory. Academic Press. New York. 376pp.

Lacarra, J.F. and O. Talagrand, 1988: Short range evolution and spectral structure of perturbations imposed on a numerical model. Tellus, 40A, 81-95.

Lepas, J., D. Rousseau, J. Coiffier, D. Carnino and R. Jourdan, 1977: Choice of a grid point model suitable for short range forecasting. GARP progress report No 15, 44-46.

Lorenc, A.C., 1981: A global three-dimensional multivariate statistical interpolation scheme. Mon. Wea. Rev., 109, 701-721.

Moll, P., 1988: Inversion variationnelle de radiances observées. Mémoire de DEA, Université de Paris 6, 54pp.

Moll, P. and Y. Durand, 1987: Application du filtre de Kalman à un modèle plan vertical en équations primitives pour l'étude de l'évolution temporelle des statistiques d'erreur. DMN/EERM Technical note No 190, 61pp.

Parrish, D., 1988: The introduction of Hough functions into optimum interpolation. Eighth conference on numerical weather prediction, Baltimore, Md. AMS, Boston.

Phillips, N.A., 1986: The spatial statistics of random geographic modes and first-guess errors. Tellus, 38A, 314-332.

Simmons, A.J., 1985: Dynamics of large scale atmospheric motion. Meteorological training course. E.C.M.W.F, Lecture Note No 1.2.

Talagrand, O. and Ph. Courtier, 1987: Variational assimilation of meteorological observations with the adjoint vorticity equation. Part I: theory. Q.J.R.M.S, 113, 1313-1330.